JOURNAL OF VIROLOGY, June 2006, p. 6115–6122 Vol. 80, No. 12
0022-538X/06/$08.00+0 doi:10.1128/JVI.00167-06

Second-Site Revertants of a Semliki Forest Virus Fusion-Block Mutation Reveal the Dynamics of a Class II Membrane Fusion Protein

Chantal Chanel-Vos† and Margaret Kielian*

Department of Cell Biology, Albert Einstein College of Medicine, Bronx, New York 10461

Received 24 January 2006/Accepted 29 March 2006

The alphavirus Semliki Forest virus (SFV) infects cells through low-pH-induced membrane fusion mediated by the E1 protein, a class II virus membrane fusion protein. During fusion, E1 inserts into target membranes via its hydrophobic fusion loop and refolds to form a stable E1 homotrimer. Mutation of a highly conserved histidine (the H230A mutation) within a loop adjacent to the fusion loop was previously shown to block SFV fusion and infection, although the mutant E1 protein still inserts into target membranes and forms a homotrimer. Here we report on second-site mutations in E1 that rescue the H230A mutant. These mutations were located in a cluster within the hinge region, at the membrane-interacting tip, and within the groove where the E1 stem is believed to pack. Together the revertants reveal specific and interconnected aspects of the fusion protein refolding reaction.

The entry of enveloped viruses into host cells requires the fusion of the viral membrane with the host cell membrane, a reaction that can occur either at the plasma membrane or in the low-pH environment of the endocytic pathway. The fusion reaction is carried out by viral membrane fusion proteins. To date, two classes of these proteins have been defined based on structural features (17). The E1 proteins of alphaviruses such as Semliki Forest virus (SFV) and the E proteins of flaviviruses such as dengue virus (DEN) and tick-borne encephalitis virus (TBE) are the current members of the class II membrane fusion proteins (reviewed in references 11, 12, 15, and 22).

The SFV fusion reaction is triggered by low pH and promoted by the presence of cholesterol in the target membrane (reviewed in references 12 and 15). During this process, the E1 fusion protein inserts into the target membrane and reorganizes into homotrimers (E1HT) that are resistant to trypsin digestion and to dissociation by sodium dodecyl sulfate (SDS) at 30°C (28, 29). The structure of the E1 ectodomain, here referred to as E1*, reveals that the prefusion form of E1 contains three domains composed almost entirely of β-sheets (17, 24). Domain I is a central globular domain that contains the E1 N terminus. Domain II is composed of two elongations that emanate from domain I. Each elongation contains a loop at its tip, the fusion peptide loop (termed the cd loop) at the tip of the first elongation and the ij loop at the tip of the second. A flexible region termed the hinge is located approximately at the boundary between domains I and II. Domain III is linked to domain I at the other side of the molecule from domain II and has a typical immunoglobulin-like fold. The stem region, a portion of which is missing in the E1* molecule, connects domain III to the transmembrane (TM) domain. In the neutral-pH conformation, the fusion peptide loop and the TM domain are present at opposite ends of the E1 molecule, and E1 is arranged tangentially to the virus membrane to form an icosahedral shell (17, 24, 31). The prefusion structure of the flavivirus E protein ectodomain shows an overall fold strikingly similar to that of SFV E1 (19, 21, 23, 32).

In the structure of the SFV low-pH-induced homotrimer (10), E1* is organized in the same domains I, II, and III, but the connections between domains are markedly altered (see Fig. 1). The E1 molecules reorient vertically to insert into the target membrane via the fusion loops at the domain II tips (8). The trimer contains an inner core composed of domains I and II. The outer layer is composed of domain III and stem, which move towards the fusion loops and interact with the groove formed by the same E1 molecule and the adjacent E1 molecule in the core trimer. In the full-length E1HT, the remaining stem region would connect to the TM domain to give a hairpin-like conformation with the fusion loop and the TM domain at the same end of the trimer, analogous to the hairpin formed by the class I fusion proteins (11, 15, 26). Inhibition by exogenous domain III demonstrated that class II membrane fusion is driven by the fold-back reaction of the fusion protein (18). Similarly to class I membrane fusion, alphavirus fusion occurs through a "hemifusion step" involving the initial mixing of the outer leaflets of the virus and target membranes (30).

Insertion of the SFV fusion loop into the target membrane was shown to require target membrane cholesterol, and thus this step appears to be primarily responsible for the cholesterol dependence of SFV fusion (1, 13, 16). Selection for growth on cholesterol-depleted insect cells was used to isolate three SFV mutants, termed *srf* (sterol requirement in function) mutants (4, 5, 27). Each mutant contains a single amino acid substitution in domain II of E1. The *srf-3* mutation is located within the ij loop adjacent to the fusion loop (27), while the *srf-4* and *srf-5* mutations are on the a and f β-strands of the hinge, respectively (4). The molecular mechanism by which these *srf* mutations affect the cholesterol requirement of E1 membrane insertion has not been defined.

Comparison of the homotrimer structure of the SFV fusion protein ectodomain with those of DEN (20) and TBE (2)

* Corresponding author. Mailing address: Department of Cell Biology, Albert Einstein College of Medicine, 1300 Morris Park Ave., Bronx, NY, 10461. Phone: (718) 430-3638. Fax: (718) 430-8574. E-mail: kielian@aecom.yu.edu.

† Present address: Weill Medical College of Cornell University, New York, NY 10021.

indicates that the overall fusion protein refolding reaction is very similar for the alphaviruses and flaviviruses, including formation of the core trimer and foldback of domain III to form the hairpin. One interesting difference is that the tips of domain II are splayed out in the SFV E1* homotrimer (E1*HT) but collapsed in the flavivirus E protein ectodomain homotrimer. This difference has been attributed to the fact that, in contrast with SFV E1*, the stem region is almost completely absent in the DEN and TBE ectodomains, which may affect the interaction and/or orientation of the fusion loops. The SFV E1*HT crystal lattice revealed interactions between the fusion loops of adjacent trimers (10). Such interactions between the fusion loops were hypothesized to produce a volcano-like hydrophobic crater that could help to bend the target membrane during the fusion reaction (10).

Here we set out to investigate the mechanism of the H230A mutation, a recently described mutation in the SFV E1 ij loop (3). H230A mutant virus is blocked in fusion and infection and is unable to carry out even the initial hemifusion step. However, the H230A mutant is fully active in both E1 interaction with the target membrane and formation of a trypsin- and SDS-resistant homotrimer, suggesting a block in a novel late intermediate in the fusion pathway (3). We selected and characterized a series of second-site revertants of the H230A mutant. The positions and properties of the rescuing mutations revealed unexpected relationships between different regions of E1 and suggested their importance in the dynamics of the class II membrane fusion reaction.

MATERIALS AND METHODS

Cells. BHK-21 cells and control and cholesterol-depleted C6/36 mosquito cells were cultured as described previously (4).

Selection of H230A revertants. Infectious RNA was prepared by in vitro transcription of the H230A infectious clone (ic) and introduced into BHK cells by electroporation (3). Viable revertants arose after incubation of infected cells for 4 to 8 days at 28°C or 2 to 4 days at 37°C. Viruses were plaque purified using agarose-containing overlays and amplified in culture at the temperature used for isolation. Virus RNAs were extracted, and the complete E1 coding sequences were obtained by reverse transcription, PCR amplification, and automated DNA sequencing (14, 25).

Growth curves. BHK cells were infected with the wild type (wt) and revertants at a multiplicity of infection of 0.01 and incubated at either 37°C or 28°C as indicated. At each time point, the viable virus present in the culture medium was quantitated either by plaque assay at 37°C or by infectious center assay at 28°C as described previously (4), using the same temperature as that used for the initial revertant isolation.

Construction of SFV H230A-*srf3*, H230A-*srf4*, and H230A-*srf5* infectious clones. Mutations were introduced into the SFV infectious clone essentially as described previously for the H230A mutant ic (3). The H230A-*srf4* double mutant was obtained by triple ligation of a BclI/SpeI fragment from the H230A ic DNA, a BclI/NsiI fragment from the *srf-4* ic DNA (4) and the NsiI/SpeI fragment from the wt ic DNA. The H230A-*srf5* double mutant was obtained by mutagenesis of the subgenomic DG-1-*srf5* clone (3, 4) with the H230A mutant primers described previously (3), followed by subcloning into the wt ic. Similarly, the H230A-*srf3* double mutant was generated by mutagenesis of wt DG-1with the following primers: 5′CTGGCACGCCCTTCATCAGGCATGGTCGCGGTAC CGTACACACAG 3′ and 5′CTGTGTGTACGGTACCGCGACCATGCCTGA TGAAGGGCGTGCCAG 3′. Two independent clones of each mutant construct, obtained from two different starting PCRs, were used to confirm initial results. Both clones for each mutant were verified by sequencing of the relevant E1 region.

Assay of E1 homotrimer formation. [^{35}S]-labeled viruses were prepared based on electroporation of wt or mutant RNA into BHK-21 cells, radiolabeling with [^{35}S]methionine-cysteine at 28°C, and purification on sucrose gradients, all as described previously (14). [^{35}S]-labeled viruses were incubated with cholesterol-containing liposomes at the indicated pH for 3 min at 37°C and then either solubilized at 30°C in SDS and analyzed by SDS-polyacrylamide gel electrophoresis (SDS-PAGE) or submitted to trypsin digestion to verify the presence of homotrimers that are not stable in SDS, as described previously (7). The E1HT was quantitated by phosphorimager analysis (Molecular Dynamics, Sunnyvale, CA), comparing the E1HT to the total (E1 plus E1HT) in each lane.

Cholesterol dependence of virus infection. The cholesterol requirement for infection by wt and mutant viruses was assessed by infection in parallel of control and cholesterol-depleted C6/36 mosquito cells. Following a 90-min infection period, cells were incubated overnight at 28°C in the presence of 20 mM NH_4Cl to prevent secondary infection. Primary infected cells were quantitated by immunofluorescence using a polyclonal rabbit antibody to the SFV envelope proteins (27).

Protein structures. The PyMOL molecular graphics system (http://www.pymol.org) (6) was used to prepare Fig. 1 and 5. The coordinates for the SFV E1* homotrimer structure (1RER) (10) are available from the Brookhaven Protein Data Bank.

TABLE 1. Pseudorevertants of the H230A mutant

Selection temp (°C)	Second-site mutation[a]	Change in nucleotide sequence[b]	No. of independent isolates
28	G83D	GGC → G**A**C	1
	L44F	TTG → TT**T**	2
	V178A	GTC → G**C**C	5
	S120P	TCT → **C**CT	1
	Q187L	CAG → C**T**G	2
	T70A	ACT → **G**CT	1
	F200L	TTC → TT**G**	
37	Q187L	CAG → C**T**G	
	S120Y	TCT → T**A**T	1
	M228I	ATG → AT**A**	
	T234R	ACA → A**G**A	1

[a] Shown are second-site mutations present in addition to the H230A mutation in the pseudorevertants. L44F is the same amino acid change found in the *srf-4* mutant, and V178A is the same amino acid change found in the *srf-5* mutant.

[b] Nucleotide changes found in the pseudorevertants are highlighted in bold.

RESULTS

Selection of H230A revertants. The H230A mutant is completely blocked in fusion and infection through a mechanism suggesting a novel late intermediate in the E1-mediated fusion reaction. Mutations that rescue the fusion defect should provide information on the late intermediate and on the overall fusion mechanism. To select for viable revertants, BHK cells were infected with the H230A mutant by electroporation with in vitro-transcribed H230A mutant RNA, and infected cells were cultured in the presence of nonelectroporated cells to allow plaque isolation of revertants (14, 25). The H230A mutant exhibits an assembly defect at 37°C that can be compensated for by incubating the infected cells at 28°C (3). Selection was therefore performed at either 28°C to select primarily for revertants that overcome the fusion defect or 37°C to select for revertants that overcome both the assembly and fusion defects. The emergence of viable revertants was monitored by plaque formation. Fourteen independent revertants were isolated and sequenced, resulting in the identification of eight revertant genotypes, six obtained from 28°C incubations and two from 37°C incubations (Table 1). None of the isolates had reverted back to the wt histidine at position 230, a change that would require the mutation of three nucleotides. Although here they will be referred to generally as "revertants," all of the isolates

are thus "second-site revertants" or "pseudorevertants" of the original H230A mutant. Interestingly, among the second-site rescuing mutations, three corresponded to mutations previously characterized in our laboratory. The most commonly isolated revertant, which was isolated five times, contained the same amino acid change as the cholesterol-independent *srf-5* mutant (V178A) (4). Another cholesterol-independent mutant, the *srf-4* mutant (L44F) (4), was isolated twice as a second-site revertant of the H230A mutant. Previous in vitro mutagenesis studies of the E1 fusion loop demonstrated that an E1 G83D mutation did not affect virus assembly, fusion efficiency, or pH dependence (25), but this mutation nonetheless was able to rescue the nonviable H230A mutant.

Locations of revertants on the E1 homotrimer structure. The fusion defect observed with the H230A mutation appears to be due to an intermediate step that lies between the formation of the membrane-inserted homotrimer and the initial lipid mixing of the viral and cellular membranes (3). To better understand how the second-site revertants rescue fusion, we analyzed each E1 change in the context of the structure of the homotrimer (Fig. 1). Three groups of second-site mutations were defined based on their locations in the E1*HT structure. (i) The first and largest group consists of mutations in the hinge region of domain II on the gfeahh′ β-sheet. The *srf-4* mutation is located on the a β-strand, the S120P mutation on the e β-strand, the *srf-5* mutation on the f β-strand, the Q187L mutation on the g β-strand, and the F200L mutation in the loop connecting β-strands g and h. Together the sites of these mutations essentially encircle the homotrimer at the hinge region (shown in Fig. 1 for one E1 molecule in the trimer). (ii) The second group is composed of mutations at the tip of domain II. This group includes a mutation in the fusion loop itself (the G83D mutation) and a mutation in the ij loop (the M228I mutation) between the lethal H230A mutation and the *srf-3* P226S mutation. (iii) The third group consists of domain II mutations located on either side of the "groove" in which the stem is believed to pack in the full-length E1HT structure. Two mutations can be put in this group, the 37°C T234R mutation in the j β-strand following the ij loop and the T70A mutation in the bc loop, which faces the T234R mutation in the adjacent E1 subunit in the homotrimer. None of the second-site mutations were located in domain I or III.

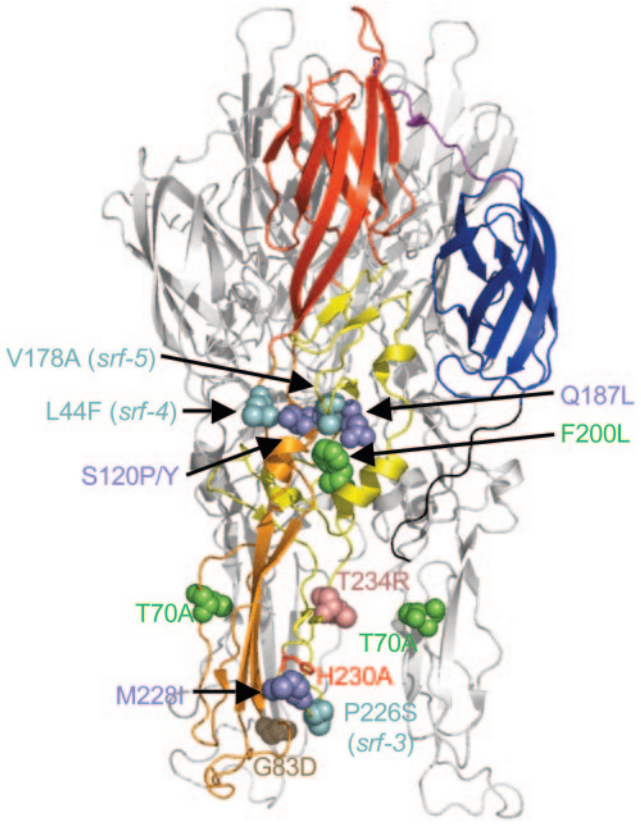

FIG. 1. Locations of second-site revertants of the H230A mutant in the E1*HT structure. Two of the three chains of the E1*HT (PDB entry 1RER) are represented in light gray, and the third chain is color-coded as follows: domain I in red, the first elongation of domain II in orange with the fusion loop at the tip, the second elongation of domain II in yellow with the cd loop at the tip, the linker between domains I and III in purple, domain III in blue, and the N-terminal portion of the stem present in the structure in black. Histidine 230 is represented as a red stick structure. Second-site mutations are represented by their van der Waals volumes and are color-coded as follows: the *srf* mutations in cyan (the *srf-4* mutation on the a β-strand, the *srf-5* mutation on the f β-strand, and the *srf-3* mutation in the ij loop), the T70A mutation (bc loop, shown on two E1 chains) and its accompanying F200L mutation (gh loop) in green, the T234R mutation (j β-strand) in pink, the G83D mutation (fusion loop) in brown, and the three mutations found in combination at 37°C (the S120Y, Q187L, and M228I mutations, on the e and g β-strands and in the ij loop, respectively) in violet-blue. Note that the S120P and Q187L mutations were also found as single second-site mutations at 28°C (Table 1). This figure was prepared using PyMOL (6).

Growth curves in BHK cells. Growth curves of all of the H230A revertants were performed to determine the extent to which the second-site revertants bypassed the H230A block in fusion and infection. To confirm the ability of the cholesterol-independent *srf-4* and *srf-5* mutations to rescue the H230A mutant, we introduced these mutations into the H230A infectious clone. These in vitro-derived mutant viruses showed phenotypes identical to those of the original revertant isolates (data not shown), confirming that the *srf-4* and *srf-5* mutations were indeed the relevant rescuing mutations. Given the high frequency of isolation of these two *srf* mutations in our revertant selection, we also tested the rescuing capacity of the *srf-3* mutation, a P226S substitution in the ij loop close to histidine 230 (27), by using mutagenesis to construct an H230A-*srf3* double mutant. For growth assays, BHK cells were infected at low multiplicity with the indicated virus stocks and incubated at the temperature originally used to isolate each revertant. At each time point, the titer of the virus in the culture media was determined on BHK cells by using an infectious center assay for the 28°C samples or a plaque assay for the 37°C samples (Fig. 2A and B, respectively). No infectious centers or plaques were produced from cells incubated in the presence of the noninfectious H230A mutant virus at either temperature (data not shown) (3). In contrast, the revertants showed growth properties at 28°C similar to those of wt SFV, with at most a decrease of about 1 log compared to the wt titer at 48 h (Fig. 2A). The H230A-*srf5* mutant grew the most efficiently, in keeping with the V178A mutation being the most frequently isolated second-site mutation. The H230A-*srf3* double mutant grew relatively poorly, presumably explaining why, although viable, it was not isolated as a pseudorevertant. The

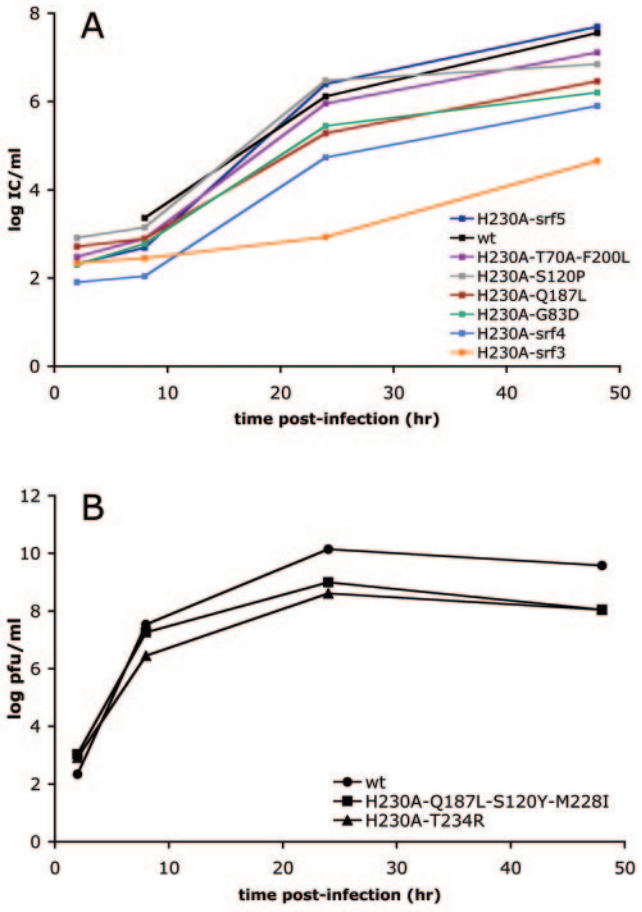

FIG. 2. Virus growth kinetics in BHK cells. BHK cells were infected with the pseudorevertants, H230A-*srf3*, or wt virus at a multiplicity of infection of 0.01 infectious centers (IC)/cell and incubated at 28°C (A) or 37°C (B) for the indicated times. At each time point, the culture media were collected and the progeny virus titers were determined by infectious center assay at 28°C (A) or plaque assay at 37°C (B). A representative example of two experiments is shown.

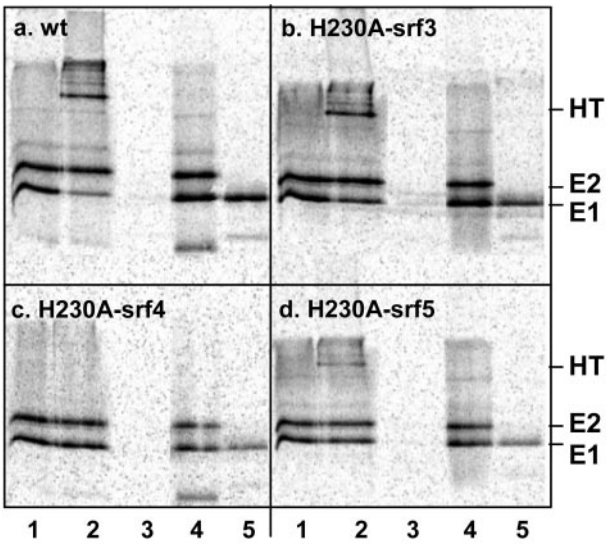

FIG. 3. Formation and stability of wt and mutant E1 homotrimers. ^{35}S-labeled wt (a), H230A-*srf3* mutant (b), H230A-*srf4* mutant (c), and H230A-*srf5* mutant (d) viruses were mixed with liposomes and treated at pH 8.0 (lanes 1 and 3) or at pH 5.5 (lanes 2, 4, and 5). The SDS resistance of the E1HT was assessed by solubilization in SDS sample buffer for 3 min at 30°C followed by SDS-PAGE (lanes 1 and 2). The trypsin resistance of the E1HT was determined by trypsin digestion (lanes 3 and 5) followed by trichloroacetic acid precipitation and detection by SDS-PAGE. Control samples (lane 4) were digested in the presence of soybean trypsin inhibitor. The positions of E1HT, E2, and E1 are indicated. A representative example of three assays of each mutant is shown.

two 37°C revertants grew with similar efficiencies, producing final titers less than 2 log lower than that of the wt (Fig. 2B). These revertants have therefore effectively compensated for both the H230A temperature-sensitive assembly defect and the H230A membrane fusion block. Only one revertant isolated at 28°C (containing the T70A and F200L second-site mutations) also regained the capacity to grow at 37°C (data not shown), and thus most of the 28°C revertants did not overcome the H230A mutation-induced assembly defect at 37°C.

Stability of the E1 homotrimer. The H230A mutant forms an E1HT with efficiency, pH dependence, and SDS stability comparable to those of the wt virus (3). The E1HTs of the *srf-4* and *srf-5* mutants were previously demonstrated to be less stable to SDS dissociation than the homotrimers of the wt, the *srf-3* mutant, or the H230A mutant (3, 4). Decreased homotrimer stability could reflect an important change in the structure of the E1HT that might play a role in the rescue of the H230A mutant fusion defect by second-site mutations. We therefore analyzed the formation and SDS stability of the E1HT for the H230A-*srf3*, H230A-*srf4*, and H230A-*srf5* double mutants. Radiolabeled viruses were mixed with liposomes, treated at pH 8.0 or at pH 5.5 to trigger low-pH-dependent conformational changes, solubilized in SDS sample buffer at 30°C, and analyzed by SDS-PAGE (Fig. 3a to d, lanes 1 and 2). Similarly to the wt virus (and the parental *srf-3* virus [not shown]), the low-pH-induced E1HT from the H230A-*srf3* mutant virus was resistant to SDS dissociation. A band migrating at the trimer position was observed, as well as more slowly migrating bands that are higher-order oligomers of the E1HT (9). By contrast, no SDS-resistant E1HT band was detectable following low-pH treatment of the H230A-*srf4* mutant and only a faint band was observed for the H230A-*srf5* mutant. Thus, the phenotypes of these two double mutants resembled those of the *srf-4* and *srf-5* parent viruses (4). To confirm the presence of the E1HT in all of the low-pH-treated samples, we evaluated the resistance of the E1 protein to trypsin digestion (7). In virus samples that had been treated at neutral pH, both the E1 and E2 proteins were completely degraded by digestion with trypsin at 37°C (Fig. 3a to d, lanes 3), in keeping with the previously described trypsin sensitivity of the pH 7 form of E1 (7). By contrast, after treatment at low pH the E1 proteins from the wt virus and the H230A-*srf3*, H230A-*srf4*, and H230A-*srf5* double mutants were all resistant to trypsin digestion (Fig. 3a to d, lanes 5), confirming generation of the E1HT. The efficiency of trypsin-resistant E1HT formation was similar for the wt and the mutants (e.g., ~50% of the total E1 converted to the homotrimer for the wt and ~40% for the H230A-*srf4* mutant). Thus, the H230A-*srf* double mutants maintained the SDS sensitivity phenotype of the original *srf* mutants. Rescue of the lethal H230A

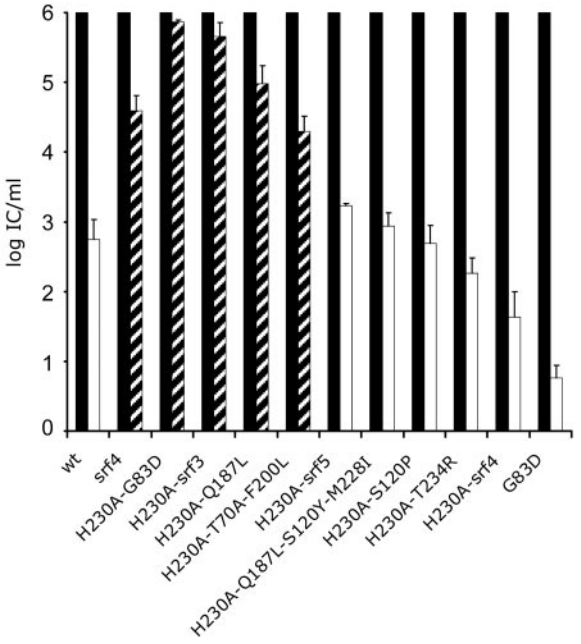

FIG. 4. Cholesterol requirements of wt and mutant SFV infection. Control (black bars) and cholesterol-depleted (hatched or white bars) C6/36 mosquito cells were infected with serial dilutions of the indicated virus stocks. The cells were then incubated overnight in the presence of NH_4Cl to prevent secondary infection, and infected cells were quantitated by immunofluorescence. The infectivity of each virus on control cells was normalized to 1×10^6 infectious centers (IC)/ml (27). Data shown are averages of two determinations with the range indicated. The hatched bars indicate mutants with a cholesterol dependence significantly lower than that of wt SFV, and the white bars indicate the wt SFV and those mutants with a significantly higher cholesterol dependence.

mutation did not require decreased SDS stability of the E1 homotrimer.

Cholesterol requirement. Strikingly, all three of the *srf* mutations previously shown to reduce the SFV cholesterol requirement for fusion were here observed to rescue the lethal H230A mutation. Thus, an alteration in viral cholesterol dependence might play an important role in the ability of a specific mutation to overcome the H230A mutant fusion defect. The cholesterol requirement for each of the pseudorevertants was therefore tested by comparing their abilities to infect control versus cholesterol-depleted C6/36 mosquito cells (Fig. 4). As previously observed (27), the wt virus infected the cholesterol-depleted cells ~3 log less efficiently than control cells. Conversely, the *srf-4* mutant showed an increase in infection of sterol-depleted cells of ~2 log compared to wt SFV, typical of the phenotype of the *srf* mutants (4). The H230A revertants showed a range of cholesterol dependence. The H230A-*srf4*, H230A-*srf5*, and H230A-S120P mutants and both pseudorevertants isolated at 37°C (the T234R and Q187L-S120Y-M228I pseudorevertants) showed a cholesterol requirement greater than or approximately equal to that of wt SFV (Fig. 4). In contrast, the H230A-G83D, H230A-*srf3*, H230A-Q187L, and H230A-T70A-F200L mutants had cholesterol dependence significantly lower than that of the wt virus (Fig. 4).

Within these two general categories of revertants, several interesting phenotypes can be discerned (Fig. 4). For the *srf* mutants, combination with the H230A mutation could cause the loss of the *srf* cholesterol-independent phenotype. For example, the *srf-4* mutant by itself was relatively cholesterol independent, but when combined with the H230A mutation the double mutant showed a cholesterol requirement even stronger than that of wt SFV, with a 4.5-log difference between the titer with cholesterol-depleted cells and that with control cells. Conversely, the G83D mutant by itself, although similar to wt SFV in growth, homotrimer formation, and fusion (25), was considerably more cholesterol dependent than the wt virus, with a difference of more than 5 log in infection of cholesterol-depleted versus control cells. However, when tested in combination with the H230A mutation the strong cholesterol requirement of the G83D mutant was nullified, resulting in almost complete cholesterol independence in the H230A-G83D revertant. An increase in cholesterol independence was also observed for the H230A-*srf3* double mutant, which was even less cholesterol dependent than the parental *srf-3* mutant. Interestingly, after several passages this virus itself rapidly reverted to a more cholesterol-dependent phenotype (data not shown). Sequence analysis of this virus isolate showed that it now contained an additional mutation, the *srf-5* V178A mutation, which conferred both more efficient growth properties and a stronger dependence on cholesterol.

The effect that the other second-site mutations would have on virus cholesterol dependence if tested in the absence of the H230A mutation is not known. Consideration of each mutation in the context of the homotrimer structure (Fig. 1) revealed that mutations within a specific region of the homotrimer, such as the hinge or the groove, could produce revertants with either a cholesterol-independent or a cholesterol-dependent phenotype. Together our data indicate that there is no correlation between the cholesterol requirement of the revertants and their capacity to rescue the H230A mutation-induced fusion defect.

DISCUSSION

We here isolated and characterized a collection of second-site revertants of the fusion-defective H230A mutant. The rescuing mutations were present in very specific regions of the E1 protein: (i) in the flexible hinge region between domain I and domain II, (ii) at the tip of domain II in either the ij or the fusion loop, and (iii) on either side of the groove in which the stem of E1 is predicted to lie in the full-length E1HT. When assayed in the wt context, several of the rescuing mutations decreased the cholesterol dependence of the SFV fusion reaction and/or the SDS stability of the homotrimer. However, neither of these properties was required for the second-site mutations to restore the fusion activity of the H230A mutant. Instead, the E1 regions that contain rescuing mutations highlight specific and interconnected aspects of the fusion reaction. Our results reveal that the hinge region can dramatically affect the function of the ij loop. They indicate an important relationship between the fusion loop and the ij loop at the membrane-interacting tip of E1. They also suggest a mechanism by which the three *srf* mutations confer common effects on the cholesterol dependence of fusion in spite of their disparate locations. More generally, consideration of how the second-

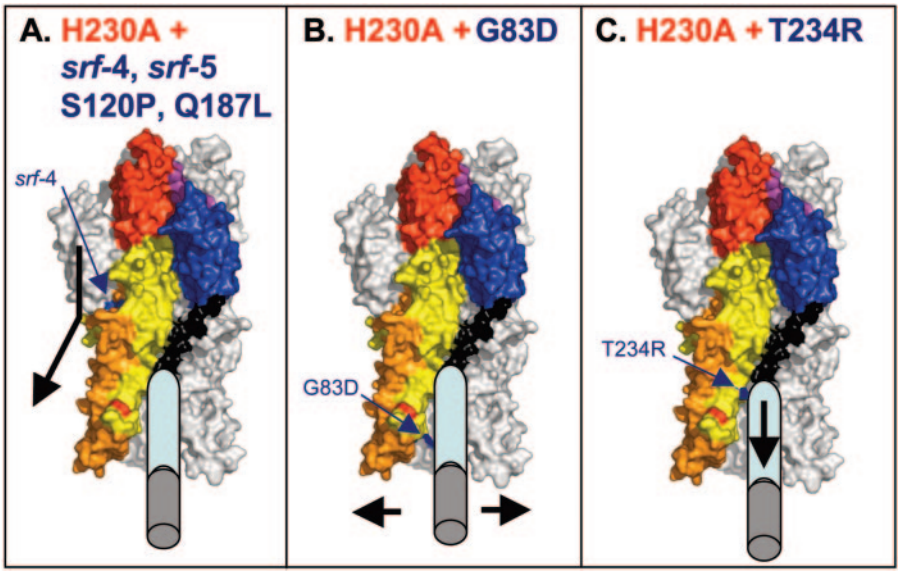

FIG. 5. Proposed model for the action of the second-site revertants of the E1 H230A mutant. The suggested mechanism for each group of revertants is illustrated using the surface representation of the SFV E1*HT structure with one monomer color-coded as in Fig. 1. The missing portion of the stem and the TM domain are represented by light-blue and dark-gray cylinders, respectively. The H230A mutation is shown in pink towards the tip of the yellow region of domain II. The second-site mutations are indicated in dark blue in each panel. (A) The hinge mutations act to change the angle of the hinge, as shown by the angled black arrow in which the angle position approximates the distance of the mutations from the domain II tip. Only the *srf-4* mutation is visible on the external trimer surface. (B) The G83D mutation acts via charge repulsion to splay apart the domain II tips, as indicated by the short black arrows. (C) The T234R mutation acts to promote the packing of the stem within the groove of the H230A mutant trimer, as indicated by the arrow on the stem.

site mutations would be expected to affect E1 refolding during homotrimer formation predicts possible mechanisms for each group of mutations that relate them to the overall fusion pathway.

Role of the hinge in class II fusion proteins. The hinge region was previously suggested to play a role in the activities of the class II fusion proteins (17, 19, 23, 32). The hinge adopts characteristic angles at different stages of virus assembly, maturation, and fusion, producing different orientations of the domain II tip relative to domain I (reviewed in reference 22). It is the site of a number of mutations that affect the pH dependence of flavivirus fusion (23) and of two of the *srf* mutations that decrease the cholesterol dependence of alphavirus fusion (4). We here demonstrate that a series of mutations located on individual β-strands in the hinge region can rescue the lethal H230A mutant fusion defect, thus providing support for an important role of the hinge in the fusion process. Two of these amino acid changes were the previously identified *srf-4* and *srf-5* mutations. The hinge is located at a considerable distance from the fusion loop, the region of E1 shown to insert into cholesterol-containing target membranes (1). The mechanism by which the two *srf* mutations in the SFV E1 hinge region affect the cholesterol dependence of SFV fusion was unknown. As discussed more fully below, the H230A revertants now suggest an important relationship between the hinge and the ij loop, where the *srf-3* mutation is located.

The domain II tip: relationship between the fusion loop and the ij loop. The available data already suggested interesting shared features of the fusion loop and the ij loop. These two loops are juxtaposed in the E1 structure both before and after fusion (10, 17, 24) and share a distinctive susceptibility to proteolytic digestion in the E1HT (9). As presented here, a mutation in the fusion loop (the G83D mutation) can rescue the H230A mutant fusion defect, strongly suggesting a functional relationship between these two E1 regions. Together the interconnections between the hinge, ij loop, and fusion loop also suggest a general model for the mechanism of the *srf* mutations. The *srf-3* mutation in the ij loop may increase the cholesterol independence of alphavirus fusion by promoting membrane insertion of the adjacent fusion loop into cholesterol-depleted target membranes. The fusion loop and the ij loop form the tips of the two elongations that extend from domain I to form domain II. The base of these two elongations is within the E1 hinge region. The presence of the *srf-4* and *srf-5* mutations in the flexible hinge region could modulate the interaction of the ij and fusion loops at the domain II tip. Thus, all of the *srf* mutations could act via effects on membrane insertion of the domain II tip.

Role of the stem region in SFV fusion. Although the C-terminal half of the stem region is missing from the SFV E1*HT structure, this region is expected to continue the stem's trajectory along the core trimer "groove" and connect to the TM domain (10). The stem-core trimer interaction was predicted to be an important part of E1 refolding during hairpin formation, with prevention of the complete fold-back reaction potentially inhibiting fusion (2, 10, 20). Since the groove is lined at its tip by the ij loop on one side and the bc loop on the other side, the packing of the stem could be disrupted by the presence of the H230A mutation in the ij loop. In this event, mutations either in the stem itself or on either side of the groove might compensate for the H230A mutation. None of

the viable revertants of the H230A mutant contained mutations in the stem region, suggesting that sequence changes in the stem cannot directly compensate for the H230A mutation or that they cause negative effects on other aspects of virus production, such as assembly (31). Two revertants did contain mutations in the groove, the T234R mutation on the j strand and the T70A mutation in the bc loop, which could potentially affect the alignment of the stem within the groove.

How do the second-site revertants rescue the alphavirus fusion reaction? The current model (10) for SFV fusion suggests that domain III folds back against the E1 core trimer and the stem region packs within a groove formed by two adjacent domains II. The optimal angle of the domain II hinge allows the splayed-out fusion loops of adjacent E1HTs to interact and organize into a volcano-like structure that induces the bending of the target membrane. The "zipping up" of domain III/stem along the core homotrimer induces an opposing dome in the virus membrane, and together these interactions induce hemifusion between the viral and target membranes, followed by full fusion.

Two possible scenarios for the effect of the H230A mutation are suggested from the available data. (i) As mentioned above, the presence of the H230A mutation in the ij loop could prevent the complete packing of the stem along the core homotrimer. (ii) Alternatively, the H230A mutation could affect the hinge and the orientation of the domain II tips to prevent correct interactions of the domain II tip with target membranes or with the tips of adjacent homotrimers. Either model (or a combination thereof) could explain why the H230A mutant virus efficiently forms the E1 homotrimer but is blocked in fusion.

Analysis of the second-site revertants suggests mechanisms by which each set could act to promote the optimal orientation of the domain II tips and/or packing of the stem inside the groove. This is presented in Fig. 5 for the revertants containing single second-site mutations. The mutations in the hinge region (Fig. 5A) presumably change the hinge angle, thus affecting the tips of domain II. Such changes could potentially also enhance the placement of the stem within the groove of the H230A mutant. Rescue by the G83D fusion loop mutation (Fig. 5B) can be explained by charge repulsion due to the insertion of a highly charged aspartate residue into the hydrophobic environment of the fusion loops, resulting in an effect on the angle of the domain II tips. Since both arginine and histidine would be positively charged at the pH of fusion, the arginine substitution at position 234 on the j strand of the T234R "groove" mutant could compensate for the loss of the H230 residue and promote packing of the stem in the groove (Fig. 5C). The T234R mutation might also affect the hinge angle.

Our results with second-site revertants of the H230A mutant thus support important roles for the hinge, ij loop, and fusion loop and identify unexpected relationships between these regions. Dominant-negative inhibition of hairpin formation has been demonstrated to inhibit class II fusion (18), but further experiments are necessary to define the dynamics of E1 refolding. Future studies should also allow us to better understand the newly described connections among the hinge, ij loop, and fusion loop and to determine their precise roles in membrane fusion and their general relevance to other class II viral fusion proteins.

ACKNOWLEDGMENTS

We thank Alice Guo for excellent technical assistance. We thank the members of our lab for helpful discussions and comments on the manuscript. The data in this paper are from a thesis submitted by C. Chanel-Vos in partial fulfillment of the requirements for the Degree of Doctor of Philosophy at the University of Paris VII.

This work was supported by a grant to M.K. from the Public Health Service (R01 GM57454) and by Cancer Center Core Support grant NIH/NCI P30-CA13330.

REFERENCES

1. **Ahn, A., D. L. Gibbons, and M. Kielian.** 2002. The fusion peptide of Semliki Forest virus associates with sterol-rich membrane domains. J. Virol. **76:** 3267–3275.
2. **Bressanelli, S., K. Stiasny, S. L. Allison, E. A. Stura, S. Duquerroy, J. Lescar, F. X. Heinz, and F. A. Rey.** 2004. Structure of a flavivirus envelope glycoprotein in its low-pH-induced membrane fusion conformation. EMBO J. **23:**728–738.
3. **Chanel-Vos, C., and M. Kielian.** 2004. A conserved histidine in the ij loop of the Semliki Forest virus E1 protein plays an important role in membrane fusion. J. Virol. **78:**13543–13552.
4. **Chatterjee, P. K., C. H. Eng, and M. Kielian.** 2002. Novel mutations that control the sphingolipid and cholesterol dependence of the Semliki Forest virus fusion protein. J. Virol. **76:**12712–12722.
5. **Chatterjee, P. K., M. Vashishtha, and M. Kielian.** 2000. Biochemical consequences of a mutation that controls the cholesterol dependence of Semliki Forest virus fusion. J. Virol. **74:**1623–1631.
6. **DeLano, W. L.** 2002. The PyMOL user's manual. DeLano Scientific, San Carlos, Calif.
7. **Gibbons, D. L., A. Ahn, P. K. Chatterjee, and M. Kielian.** 2000. Formation and characterization of the trimeric form of the fusion protein of Semliki Forest virus. J. Virol. **74:**7772–7780.
8. **Gibbons, D. L., I. Erk, B. Reilly, J. Navaza, M. Kielian, F. A. Rey, and J. Lepault.** 2003. Visualization of the target-membrane-inserted fusion protein of Semliki Forest virus by combined electron microscopy and crystallography. Cell **114:**573–583.
9. **Gibbons, D. L., and M. Kielian.** 2002. Molecular dissection of the Semliki Forest virus homotrimer reveals two functionally distinct regions of the fusion protein. J. Virol. **76:**1194–1205.
10. **Gibbons, D. L., M.-C. Vaney, A. Roussel, A. Vigouroux, B. Reilly, J. Lepault, M. Kielian, and F. A. Rey.** 2004. Conformational change and protein-protein interactions of the fusion protein of Semliki Forest virus. Nature **427:**320–325.
11. **Harrison, S. C.** 2005. Mechanism of membrane fusion by viral envelope proteins. Adv. Virus Res. **64:**231–261.
12. **Kielian, M.** 2006. Class II virus membrane fusion proteins. Virology **344:** 38–47.
13. **Kielian, M., P. K. Chatterjee, D. L. Gibbons, and Y. E. Lu.** 2000. Specific roles for lipids in virus fusion and exit: examples from the alphaviruses, p. 409–455. *In* H. Hilderson and S. Fuller (ed.), Subcellular biochemistry, vol. 34. Fusion of biological membranes and related problems. Plenum Publishers, New York, N.Y.
14. **Kielian, M., M. R. Klimjack, S. Ghosh, and W. A. Duffus.** 1996. Mechanisms of mutations inhibiting fusion and infection by Semliki Forest virus. J. Cell Biol. **134:**863–872.
15. **Kielian, M., and F. A. Rey.** 2006. Virus membrane fusion proteins: more than one way to make a hairpin. Nat. Rev. Microbiol. **4:**67–76.
16. **Klimjack, M. R., S. Jeffrey, and M. Kielian.** 1994. Membrane and protein interactions of a soluble form of the Semliki Forest virus fusion protein. J. Virol. **68:**6940–6946.
17. **Lescar, J., A. Roussel, M. W. Wien, J. Navaza, S. D. Fuller, G. Wengler, and F. A. Rey.** 2001. The fusion glycoprotein shell of Semliki Forest virus: an icosahedral assembly primed for fusogenic activation at endosomal pH. Cell **105:**137–148.
18. **Liao, M., and M. Kielian.** 2005. Domain III from class II fusion proteins functions as a dominant-negative inhibitor of virus-membrane fusion. J. Cell Biol. **171:**111–120.
19. **Modis, Y., S. Ogata, D. Clements, and S. C. Harrison.** 2003. A ligand-binding pocket in the dengue virus envelope glycoprotein. Proc. Natl. Acad. Sci. USA **100:**6986–6991.
20. **Modis, Y., S. Ogata, D. Clements, and S. C. Harrison.** 2004. Structure of the dengue virus envelope protein after membrane fusion. Nature **427:**313–319.
21. **Modis, Y., S. Ogata, D. Clements, and S. C. Harrison.** 2005. Variable surface epitopes in the crystal structure of dengue virus type 3 envelope glycoprotein. J. Virol. **79:**1223–1231.

22. **Mukhopadhyay, S., R. J. Kuhn, and M. G. Rossmann.** 2005. A structural perspective of the flavivirus life cycle. Nat. Rev. Microbiol. **3:**13–22.
23. **Rey, F. A., F. X. Heinz, C. Mandl, C. Kunz, and S. C. Harrison.** 1995. The envelope glycoprotein from tick-borne encephalitis virus at 2A resolution. Nature **375:**291–298.
24. **Roussel, A., J. Lescar, M.-C. Vaney, G. Wengler, G. Wengler, and F. A. Rey.** 2006. Crystal structure of the Semliki Forest virus envelope protein E1 in its monomeric conformation: identification of determinants for icosahedral particle formation. Structure **14:**75–86.
25. **Shome, S. G., and M. Kielian.** 2001. Differential roles of two conserved glycine residues in the fusion peptide of Semliki Forest virus. Virology **279:**146–160.
26. **Skehel, J. J., and D. C. Wiley.** 2000. Receptor binding and membrane fusion in virus entry: the influenza hemagglutinin. Annu. Rev. Biochem. **69:**531–569.
27. **Vashishtha, M., T. Phalen, M. T. Marquardt, J. S. Ryu, A. C. Ng, and M. Kielian.** 1998. A single point mutation controls the cholesterol dependence of Semliki Forest virus entry and exit. J. Cell Biol. **140:**91–99.
28. **Wahlberg, J. M., R. Bron, J. Wilschut, and H. Garoff.** 1992. Membrane fusion of Semliki Forest virus involves homotrimers of the fusion protein. J. Virol. **66:**7309–7318.
29. **Wahlberg, J. M., and H. Garoff.** 1992. Membrane fusion process of Semliki Forest virus I: low pH-induced rearrangement in spike protein quaternary structure precedes virus penetration into cells. J. Cell Biol. **116:**339–348.
30. **Zaitseva, E., A. Mittal, D. E. Griffin, and L. V. Chernomordik.** 2005. Class II fusion protein of alphaviruses drives membrane fusion through the same pathway as class I proteins. J. Cell Biol. **169:**167–177.
31. **Zhang, W., S. Mukhopadhyay, S. V. Pletnev, T. S. Baker, R. J. Kuhn, and M. G. Rossmann.** 2002. Placement of the structural proteins in Sindbis virus. J. Virol. **76:**11645–11658.
32. **Zhang, Y., W. Zhang, S. Ogata, D. Clements, J. H. Strauss, T. S. Baker, R. J. Kuhn, and M. G. Rossmann.** 2004. Conformational changes of the flavivirus E glycoprotein. Structure (Cambridge) **12:**1607–1618.